

Using $(1 + 1)D$ quantum cellular automata for exploring collective effects in large-scale quantum neural networks

Edward Gillman^{1,2}, Federico Carollo³, and Igor Lesanovsky^{1,2,3}

¹*School of Physics and Astronomy, University of Nottingham, Nottingham NG7 2RD, United Kingdom*

²*Centre for the Mathematics and Theoretical Physics of Quantum Non-Equilibrium Systems, University of Nottingham, Nottingham NG7 2RD, United Kingdom*

³*Institut für Theoretische Physik, Universität Tübingen, Auf der Morgenstelle 14, 72076 Tübingen, Germany*



(Received 5 August 2022; accepted 13 January 2023; published 22 February 2023)

Central to the field of quantum machine learning is the design of quantum perceptrons and neural network architectures. A key question in this regard is the impact of quantum effects on the way such models process information. Here, we establish a connection between $(1 + 1)D$ quantum cellular automata, which implement a discrete nonequilibrium quantum many-body dynamics through successive applications of local quantum gates, and quantum neural networks (QNNs), which process information by feeding it through perceptrons interconnecting adjacent layers. Exploiting this link, we construct a class of QNNs that are highly structured—aiding both interpretability and helping to avoid trainability issues in machine learning tasks—yet can be connected rigorously to continuous-time Lindblad dynamics. We further analyze the universal properties of an example case, identifying a change of critical behavior when quantum effects are varied, showing their potential impact on the collective dynamical behavior underlying information processing in large-scale QNNs.

DOI: [10.1103/PhysRevE.107.L022102](https://doi.org/10.1103/PhysRevE.107.L022102)

An established concept for classifying phases of matter and transitions among them is that of universality. This builds on the observation that, near a critical point, different systems display macroscopic behavior that does not depend on their microscopic details [1]. Consequently, a wide variety of systems exhibit the same collective scaling behavior for key observables. In equilibrium this can be observed, e.g., in the magnetization of the Ising model and the specific volume of a van der Waals gas, both of which follow the same scaling laws near the critical point. In the realm of nonequilibrium phase transitions (NEPTs) universality can be, for instance, observed in dynamical processes that feature an absorbing state—a particular configuration of the system which, once reached, causes the dynamics to halt. These systems feature emergent collective behavior that typically belongs to the so-called directed percolation (DP) universality class. This is, e.g., the case for both the continuous-time classical contact process (CCP) [2,3] and the discrete-time Domany-Kinzel cellular automata (DKCA) [3–9], which, despite their very different microscopic formulation, display the same quantitative large-scale critical physics. We note that this concept of *physical* universality is separate from other conceptions of universality, such as *computational* universality which is important in the field of information processing, though the question of how such concepts can relate is an interesting one in its own right, particularly in physically inspired models of computation such as cellular automata [10].

Recently, it has been found that quantum effects can lead to a change of the universal behavior of nonequilibrium stochastic processes. This has been observed in a continuous-time open quantum version of the contact process model [11–16],

with a similar change also found within so-called $(1 + 1)D$ quantum cellular automata (QCA) [17] [see Fig. 1(a)]. QCA represent an extension of classical cellular automata (CCA) into the quantum domain [18–22] and can, for instance, be realized on quantum hardware based on Rydberg atoms [23–27]. Moreover, QCA are also closely related to quantum neural networks (QNNs) [see Fig. 1(a)], which are of considerable interest in current quantum machine learning research [28–31]. This interest is driven by the idea that QNNs might accomplish learning tasks related to quantum data more efficiently than their classical counterparts [32].

Building on the connection between $(1 + 1)D$ QCA and a paradigmatic class of QNNs [17,28], we address the question of how information processing in *large* QNNs can be analyzed through the lens of quantum dynamics, and how quantum effects can dramatically alter the dynamical behavior in QNNs designed for application to quantum machine learning (QML) tasks. To this end, we first introduce a class of quantum perceptrons (gates) that provide highly structured (few parameter) QNNs, whose information processing can be interpreted clearly as a dissipative many-body quantum dynamics that is equivalent to generic continuous-time Markovian open quantum time evolutions in a particular limit. In the field of QML, similar highly structured models have recently shown promise in the task of (unitary) dynamics learning [33]. Not only does the nature of these models make them easy to interpret in terms of physical dynamics, it has also been suggested that their structure can aid trainability [34], an issue that is faced by more general unrestricted QNNs [31,35]. This then provides the motivation for the restricted class of QNNs presented here as potential interpretable models for

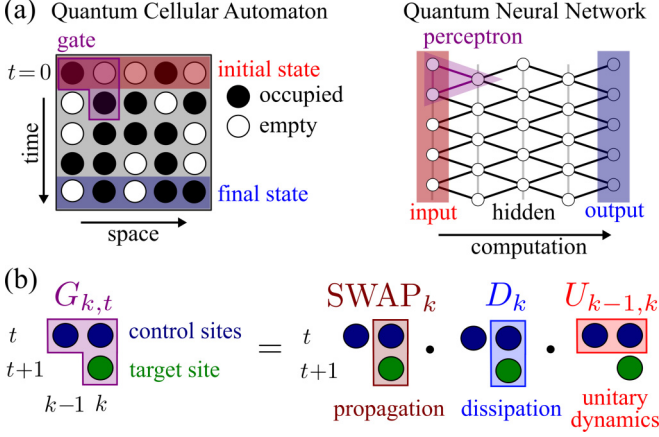


FIG. 1. QCA and QNNs. (a) $(1+1)D$ QCA propagate an initial quantum state, defined on a one-dimensional lattice, along a discrete-time direction via the application of quantum gates. First, one applies the gates successively to all qubits (sites) of a given row. This completes one time step and one subsequently advances to the next row. This discrete time evolution is closely related to the dynamics of a computation on a recurrent QNN. Here information is processed by perceptrons that link adjacent layers, thereby propagating the input (initial state) to the output (final state). (b) We consider a gate $G_{k,t}$ with two control qubits (on time slice t) and one target qubit (on time slice $t+1$). For the shown decomposition of the gate one obtains an effective open system dynamics (with single-site dissipation) through unitary gates: first, a unitary $U_{k-1,k}$ is applied to control qubits, which implements a Hamiltonian evolution. Second, an entangling gate D_k acts on one of the controls and on the target qubit, resulting in dissipation. Finally, a propagation step which is implemented by applying a swapping operation, SWAP_k , between control and target qubits.

the learning of Lindblad (nonunitary) dynamics. Finally, we exploit the QNN-QCA connection again to investigate the impact of quantum effects on collective behavior. To do this, we focus on a case where the QNN (taken from the class established previously) has a dynamics displaying an NEPT. Using numerical simulations based on tensor networks (TNs), we investigate long propagation times, corresponding to deep QNNs, and large system sizes, corresponding to a large number of neurons per layer. We find that, indeed, quantum fluctuations can impact on emergent properties within QNNs, i.e., as a function of the parameters of the perceptrons they lead to changes in the universal critical dynamics.

Relationship between QCA and QNNs. A $(1+1)D$ QCA consists of a two-dimensional lattice of sites, each one having as basis states an *empty* one, $|\circ\rangle$, and an *occupied* one, $|\bullet\rangle$. Similar to CCA, the whole lattice is prepared with all sites in state $|\circ\rangle$, apart from those in the first row, here denoted as row $t=0$ as shown in Fig. 1(a). The latter encode the initial state of an effective one-dimensional system, such as a chain of L two-level systems, where L is the width of the lattice. The state of $(1+1)D$ QCA then evolves iteratively as $|\psi_{t+1}\rangle = \mathcal{G}_t |\psi_t\rangle$, where \mathcal{G}_t is a global-update operator defined via the application of local (unitary) gates $G_{k,t}$, $\forall k$. Each $G_{k,t}$ acts on a set of so-called control sites in the neighborhood of site k in row t and on the target site k in row $t+1$ [see an example in Fig. 1(b)]. The successive update of consecutive

rows allows one to interpret the vertical dimension of the lattice [cf. Fig. 1(a)] as an effective time dimension for the evolution of the one-dimensional system encoded in the QCA. Its (reduced) state, at time t , is given by the density matrix $\rho(t) = \text{Tr}_t[|\psi_t\rangle\langle\psi_t|]$, with Tr_t indicating trace over all sites but those in row t . Since \mathcal{G}_t acts nontrivially only on two adjacent rows, the (reduced) dynamics of $\rho(t)$ is given by

$$\rho(t+1) = \text{Tr}_{t+1}[\mathcal{G}_t \rho(t) \otimes |0\rangle\langle 0|_{t+1} \mathcal{G}_t^\dagger], \quad (1)$$

where $|0\rangle_{t+1}$ is the state of row $t+1$, initialized with all (target) sites in $|\circ\rangle$. In order not to overload the notation, we will use here the symbol \mathcal{G}_t to indicate both the full unitary operator and its reduced form solely supported on row t and $t+1$.

As illustrated in Fig. 1(a), $(1+1)D$ QCA are structurally equivalent to layered QNNs composed of perceptrons [28,31]. The input layer of the QNN is the initial state of the one-dimensional system encoded in the QCA, while the remaining nodes of the network, i.e., those in the hidden layers and in the output layer, are initialized in the *fiduciary* state $|\circ\rangle$. The (neural) nodes of two adjacent layers are connected by (unitary) perceptrons, which are implemented by the application of the gate \mathcal{G}_t in the QCA. In the context of QNNs, the time dimension of the QCA represents a direction quantifying the progress of a computation, and the state at the output layer corresponds to the state $\rho(t)$ of the QCA, as defined in Eq. (1), at a chosen final time [cf. Fig. 1(a)]. Since we consider here gates $G_{k,t}$ which are identical for all t and k , our QCA in fact reproduces a recurrent QNN [34].

Information processing through dissipative quantum dynamics. As discussed above, $(1+1)D$ QCA, and thus also QNNs, encode a discrete-time dynamics [cf. Eq. (1)]. Here, we introduce a class of gates (perceptrons), $G_{k,t}$, for which, in a given limit of their parameters, this dynamics becomes equivalent to a continuous-time many-body open quantum system evolution. This is of potential interest for the learning of dissipative quantum dynamics, with similar highly structured perceptrons having proved important for learning closed, Hamiltonian dynamics [34]. However, this construction also enables the examination of the information processing of QNNs in terms of equivalent dynamical properties (see, e.g., Ref. [36]).

The dissipative quantum dynamics we will consider is described by the so-called Lindblad generator [37]

$$\mathcal{L}[\rho] = -i[H, \rho] + \sum_{\mu} (J_{\mu} \rho J_{\mu}^\dagger - \frac{1}{2} \{J_{\mu}^\dagger J_{\mu}, \rho\}). \quad (2)$$

Here the commutator term, which includes the Hamiltonian H , gives rise to a coherent quantum evolution, while the dissipator, which depends on the jump operators J_{μ} , encodes a nonreversible (classical) process. For the sake of concreteness, we consider a QCA with gates $G_{k,t}$ acting on two control sites and a single target site, as is the case for the gate shown in Fig. 1(b). Generalizations to more control sites are straightforward.

In order for the dynamics in Eq. (1) to be (approximately) equivalent to the continuous-time dynamics generated by \mathcal{L} , we require that $\rho(t+1) \approx \rho(t) + \delta t \mathcal{L}[\rho(t)]$, where δt is a small, as compared to the timescales of the system, time increment. This can be achieved (see Supplemental Material

[38]) via a global-update operator \mathcal{G}_t , composed of local gates [cf. Fig. 1(b)]

$$G_{k,t} = \text{SWAP}_k D_k U_{k-1,k}, \quad (3)$$

applied in a right-to-left sweep gate ordering. Here, $U_{k-1,k} = e^{-i\delta t h_{k-1,k}}$ (with the special case $U_{0,1} = \mathbb{I}$, i.e., open boundary conditions) unitarily evolves the control sites $k-1, k$ with the local Hamiltonian $h_{k-1,k}$. The operator D_k , given by

$$D_k = \exp[i\theta(\sigma_k^+ \otimes \sigma_k^- + \sigma_k^- \otimes \sigma_k^+)], \quad (4)$$

with $\sigma^- = (\sigma^+)^\dagger = |\circ\rangle\langle\bullet|$, generates entanglement between the control site (k, t) and the target site $(k, t+1)$ which results in dissipation in the form of local decay from state $|\bullet\rangle$ to state $|\circ\rangle$ at site k . The parameter θ needs to be small in order to approximate a continuous-time update. For small δt , we assume $\theta \approx \sqrt{\gamma\delta t}$, where γ provides the decay rate. Finally, the operator SWAP_k performs a swap of site (k, t) with site $(k, t+1)$, which is needed to advance the state of the system to the next row. Note that, in the case of a fully coherent Hamiltonian evolution one has $D_k = \mathbb{I}$, and the target sites become redundant [39–43].

In order to see that using the local gates in Eq. (3) gives rise to a continuous-time Lindblad dynamics, we consider Eq. (1), which in the present case reads [38]

$$\rho(t+1) = \sum_m \mathcal{K}_m U_t \rho(t) U_t^\dagger \mathcal{K}_m^\dagger. \quad (5)$$

Here, $m = (m_1, m_2, \dots, m_L)$, with $m_k = \circ, \bullet$ labeling the basis states. The operator $U_t = \prod_k U_{k-1,k}$ implements the full unitary update, while $\mathcal{K}_m = \prod_k \mathcal{K}_{m_k,k}$, with $\mathcal{K}_{m_k,k} = \langle m_k | D_k | \circ \rangle$, are the (Kraus) operators associated with local decay. Recalling Eq. (4), one has

$$\mathcal{K}_{\circ,k} = \mathbb{I} + [\cos(\theta) - 1] n_k, \quad \mathcal{K}_{\bullet,k} = i \sin(\theta) \sigma_k^-, \quad (6)$$

where $n = |\bullet\rangle\langle\bullet|$. For small angles $\theta \approx \sqrt{\gamma\delta t} \ll 1$, we can expand the Kraus operators \mathcal{K}_m in powers of δt . Up to first order in δt , in Eq. (5) one has at most a single $m_k = \bullet$. Since this can happen for all k , the sum of these contributions leads to a term equivalent to the first sum in Eq. (2), acting on $U_t \rho(t) U_t^\dagger$. Expanding the term with all $m_k = \circ$ in Eq. (5) gives instead the second sum in Eq. (2) applied to $U_t \rho(t) U_t^\dagger$ as well as the contribution $U_t \rho(t) U_t^\dagger$ itself. Finally, expanding also the $U_{k-1,k}$ up to first order in δt , gives rise to a Lindblad operator which has the form of Eq. (2), with Hamiltonian $H = \sum_k h_{k-1,k}$ and jump operator $J_k = \sqrt{\gamma} \sigma_k^-$.

Emergent collective many-body behavior. Having shown that QNNs effectively implement open quantum dynamics, we exploit this connection to investigate emergent quantum many-body behavior in large-scale QNNs. To this end, we focus on a scenario in which critical behavior associated with an NEPT can be observed. We achieve this by considering a Hamiltonian with $h_{k,k+1} = \Omega(\sigma_k^y n_{k+1} + n_k \sigma_{k+1}^y)$ and $\sigma^y = -i|\bullet\rangle\langle\circ| + \text{H.c.}$, which establishes coherent oscillations between the two states of a given site only if at least one of the neighboring sites is in state $|\bullet\rangle$, e.g., $|\circ\bullet\rangle \leftrightarrow |\bullet\bullet\rangle$, a process which can be interpreted as quantum branching and coagulation. The reason for this choice is that, in combina-

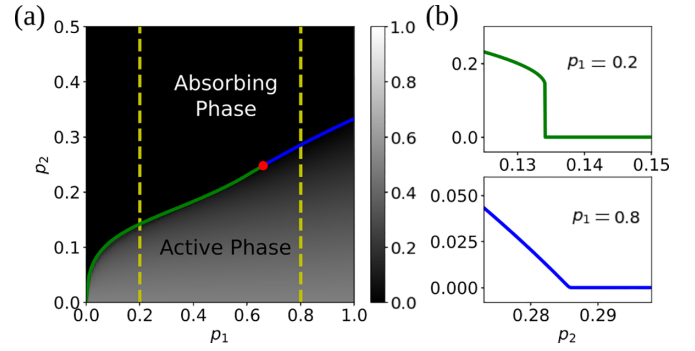


FIG. 2. Mean-field phase diagram: (a) Mean-field estimate for the stationary value of $\langle n \rangle$. To estimate the critical line, the gradient along each p_1 slice was calculated, and the point of maximum absolute gradient taken as the estimate for the critical p_2 value. The transition is estimated to be continuous when this gradient is below a threshold, set here to 10 (the number of sampling points in the p_2 direction is 2001), and discontinuous otherwise. The separating “transition point” is indicated by a red circle. (b) Two slices are shown for $p_1 = 0.2, 0.8$. For these, the mean-field equations were iterated over $T = 10\,000$ steps. For $p_1 = 0.2$, one can clearly observe a discontinuity in the stationary value of $\langle n \rangle$.

tion with local decay, it gives rise in the small δt limit to the so-called quantum contact process (QCP), theoretically studied in Refs. [14,16], and recently experimentally explored in Ref. [44]. The ensuing dynamics displays an NEPT into an absorbing state (with all sites in $|\circ\rangle$) and emergent critical behavior influenced by quantum effects [14]. Due to universality, this phase transition also emerges when δt is not small, which is certainly the case in a generic QNN, where the gates $G_{k,t}$ implement discrete updates.

To systematically analyze this model, we reparametrize it as follows: $\theta = \arcsin(p_2)$, with $p_2 = \sin^2(\sqrt{\gamma\delta t}/2)$ and $\Omega\delta t = (1/\sqrt{2}) \arcsin \sqrt{p_1}$. The two real parameters $p_1, p_2 \in [0, 1]$ can be interpreted as probabilities associated with the transitions $|\circ\bullet\rangle \leftrightarrow |\bullet\bullet\rangle$ due to the coherent branching and coagulation, and with the local decay $|\bullet\rangle \rightarrow |\circ\rangle$, respectively. The continuous-time dynamics in Eq. (2) is then reproduced by Eq. (1) when taking $p_1, p_2 \rightarrow 0$, for which $\delta t \rightarrow 0$.

Mean-field analysis. To investigate how quantum effects manifest in emergent behavior of large-scale QNNs, we study the stationary behavior of the associated QCA and look for signatures of NEPTs and critical behavior. We first derive the stationary phase diagram through a mean-field analysis, which allows us to gain insight on its overall structure [18,19,21] (see [38] for details).

In Fig. 2(a) we show the mean-field phase diagram. When p_2 is sufficiently large (large decay probability), the state $\rho(t)$ converges towards a stationary one with zero density of sites in the state $|\bullet\rangle$, i.e., $\langle n \rangle = 0$. This phase is known as absorbing phase. On the other hand, for sufficiently small p_2 , the stationary density $\langle n \rangle$ can be finite, $\langle n \rangle > 0$. This establishes the existence of an active phase. The phase transition between these two regions appears discontinuous when $p_1 \lesssim 0.66$ and continuous otherwise [see Fig. 2(b)]. When $p_1 = 1$, the mean-field equation for the density of occupied sites can be explicitly solved [38] giving solutions $\langle n \rangle = 0$ as

well as

$$\langle n \rangle = \frac{3}{2} + \frac{1}{p_2 - 1}. \quad (7)$$

This second solution vanishes continuously approaching $p_2 \rightarrow 1/3$ from above. This behavior is similar to that expected from a (mean-field) NEPT in the DP universality class, which is displayed by the CCP, i.e., the classical version of the contact process in which branching and coagulation occur as incoherent nonreversible processes.

These findings show that a large QNN can indeed display emergent collective behavior akin to that of an NEPT. For $p_1 = 1$, it appears that the QNN/QCA, as constructed here, exhibits classical collective behavior. However, reducing the value of p_1 changes the nature of the phase transition phenomenology, from a continuous to a first-order one. A similar phenomenon was identified in an open quantum contact process model with competing classical (incoherent) and quantum (coherent) branching and coagulation [11]. There, the discontinuous mean-field transition turns out to in fact be a continuous NEPT whose universal exponents are different from DP due to quantum effects [14]. This suggests that quantum fluctuations indeed can impact on the processing of information and concomitant collective effects in QNNs.

Tensor-network analysis. To confirm that tuning p_1 indeed changes the NEPT, we employ (nonperturbative) TN methods. The approach taken here follows that of Ref. [21], and directly approximates the evolution of $\rho(t)$ in a vectorized representation. We consider an initial state with all sites in $|\bullet\rangle$ and the evolution of the density $\langle n \rangle$ up to $T = 100$ time steps.

The first task is to estimate the position of the critical line separating the active phase and the absorbing phase. To this end, we take two different approaches, both exploiting that $\langle n(t) \rangle$ obeys a power-law behavior in time on the critical line. This means that, at criticality, $\langle n(t) \rangle \sim t^{-\alpha}$, where α is a dynamical exponent characterizing the universal behavior of the model. Details on the methods employed are given in [38].

As shown in Fig. 3, the TN phase diagram qualitatively agrees with the mean-field one, although the active phase seems to extend to higher values of p_2 in the latter case. In order to gain insights on the critical behavior of the model, we analyze the critical exponent α by investigating the behavior of the effective exponent $\alpha(t) = -\log_2 \langle n(2t) \rangle / \langle n(t) \rangle$. The latter becomes constant for exact power laws, in which case it further provides an estimate for α (see Ref. [38] for details).

As shown in the inset of Fig. 3, while the precise estimation of α and associated errors is challenging, for $p_1 \leq 0.5$, the obtained value of the exponent always lies far from the 1D DP value $\alpha_{\text{DP}} \approx 0.16$, and is in fact close to that of the 1D QCP, $\alpha_{\text{QCP}} = 0.32$ [14]. This suggests that, despite being far from the continuous-time limit, the dynamics displays the same critical behavior as the QCP and, unlike the CCP, does not fall into the DP universality class. However, as shown in the inset, errors, particularly due to finite-size effects, increase with p_1 and determining the universality class in this regime becomes more and more challenging. It is therefore difficult to reliably estimate a particular location where the universality class changes from that of the QCP to DP. This issue is compounded

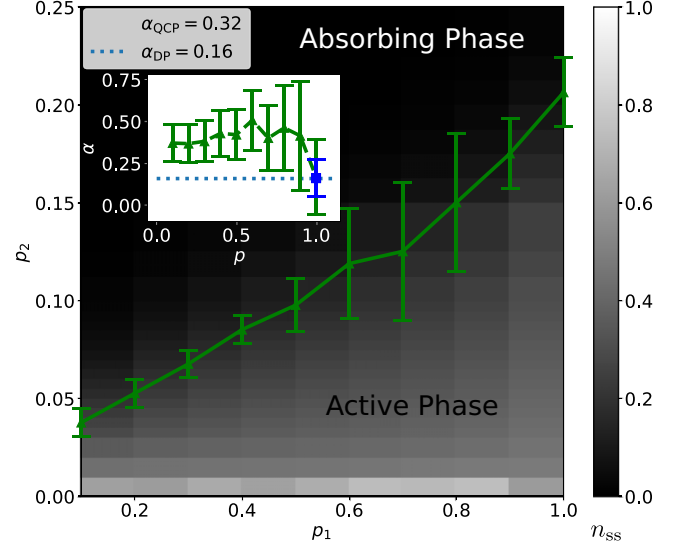


FIG. 3. Tensor-network phase diagram: The density $\langle n \rangle$ is estimated by evolving $\rho(t)$ over $T = 100$ steps, with a bond dimension of $\chi = 512$, lattice size of $L = 128$, and starting from a fully occupied state. The critical line shown in green (triangles) is estimated by taking the average of two estimates, one using linear fits of $\langle n(t) \rangle$ in a log-log scale, and another using an effective exponent $\alpha(t)$ (see [38] for details). The error bars combine the two errors on these estimated values of p_2 (each induced by the resolution of the parameter grid). The inset shows the corresponding critical exponents (green triangles), obtained by averaging $\alpha(t)$ over $t \in [80, 100]$. Errors occurring on each effective exponent separately are indicated by the error bars and involve contributions from finite sizes, finite bond dimensions, and finite parameter grid resolutions [38]. As can be seen, errors tend to increase with p_1 . To gain a higher accuracy estimate of the exponent for $p_1 = 1$, the procedure was repeated with $L = 256$ (blue square in the inset). The dotted (dashed) line shows the exponent α expected for the DP (QCP) universality class.

by the suggestion that, in fact, due to the competition between quantum and classical effects, the dynamical exponent may even vary continuously [16]. As such, we here consider the extreme point $p_1 = 1$ and run a finer parameter scan with a larger system size to reduce errors. The resulting estimate for the critical exponent lies very close to that of 1D DP (cf. inset of Fig. 3), indicating that indeed the universality class must change at some point, as suggested by the mean-field analysis.

Summary and outlook. We have established a connection between perceptron-based QNNs and $(1+1)D$ QCA, which emerge as natural generalizations of CCA for the study of quantum nonequilibrium processes. This connection allows the processing of information in QNNs to be linked to many-body quantum dynamics. We have introduced a class of highly structured few-parameter QNN architectures, suitable, e.g., for applications to QML for nonunitary dynamics, and shown how these can encode continuous-time open quantum dynamics in a certain limit. By building on the quantum and classical versions of the contact processes—many-body systems whose collective properties are altered by quantum effects—we demonstrated that indeed universal (detail-independent) dynamical properties of information processing in QNNs can quantitatively change by the prevalence of quantum fluctu-

ations. A natural future avenue for investigation is into the trainability of the class of QNNs introduced here, and the establishment of performance benchmarks for QML tasks such as nonunitary dynamics learning. Such studies can be conducted, e.g., within the recently introduced TensorFlow Quantum programming framework [34]. Furthermore, with recent studies examining the scaling of quantum correlations during NEPTs in model architectures such as the one presented here [21], the present work also provides a promising foundation for investigating the relationship between quantum correlations and performance on information processing tasks in QNNs more generally.

Acknowledgments. We are grateful to Markus Müller and Mario Boneberg for fruitful discussions. We acknowledge support from EPSRC (Grant No. EP/V031201/1), from the “Wissenschaftler Rückkehrprogramm GSO/CZS” of the Carl-Zeiss-Stiftung and the German Scholars Organization e.V., through The Leverhulme Trust (Grant No. RPG-2018-181), and the Deutsche Forschungsgemeinschaft through Grants No. 449905436 and No. 435696605 as well as through the Research Unit FOR 5413/1, Grant No. 465199066 and Germany’s Excellence Strategy – EXC-Number 2064/1 – Project No. 390727645. We are grateful for access to the University of Nottingham’s Augusta HPC service.

-
- [1] N. Goldenfeld, *Lectures on Phase Transitions and the Renormalization Group* (CRC Press, Boca Raton, FL, 2018).
 - [2] T. E. Harris, *Ann. Prob.* **2**, 969 (1974).
 - [3] M. Henkel, H. Hinrichsen, and S. Lübeck, *Non-Equilibrium Phase Transitions* (Springer, Netherlands, 2008).
 - [4] M. Henkel and M. Pleimling, *Non-Equilibrium Phase Transitions* (Springer, Netherlands, 2010).
 - [5] E. Domany and W. Kinzel, *Phys. Rev. Lett.* **53**, 311 (1984).
 - [6] F. Bagnoli, N. Boccara, and R. Rechtman, *Phys. Rev. E* **63**, 046116 (2001).
 - [7] F. Bagnoli and R. Rechtman, [arXiv:1409.4284](https://arxiv.org/abs/1409.4284).
 - [8] H. Hinrichsen, *Adv. Phys.* **49**, 815 (2000).
 - [9] S. Lübeck, *Int. J. Mod. Phys. B* **18**, 3977 (2004).
 - [10] R. A. Meyers, *Encyclopedia of Complexity and Systems Science* (Springer, New York, 2009).
 - [11] M. Marcuzzi, M. Buchhold, S. Diehl, and I. Lesanovsky, *Phys. Rev. Lett.* **116**, 245701 (2016).
 - [12] M. Buchhold, B. Everest, M. Marcuzzi, I. Lesanovsky, and S. Diehl, *Phys. Rev. B* **95**, 014308 (2017).
 - [13] D. Roscher, S. Diehl, and M. Buchhold, *Phys. Rev. A* **98**, 062117 (2018).
 - [14] F. Carollo, E. Gillman, H. Weimer, and I. Lesanovsky, *Phys. Rev. Lett.* **123**, 100604 (2019).
 - [15] E. Gillman, F. Carollo, and I. Lesanovsky, *New J. Phys.* **21**, 093064 (2019).
 - [16] M. Jo, J. Lee, K. Choi, and B. Kahng, *Phys. Rev. Res.* **3**, 013238 (2021).
 - [17] E. Gillman, F. Carollo, and I. Lesanovsky, *Phys. Rev. E* **106**, L032103 (2022).
 - [18] I. Lesanovsky, K. Macieszczak, and J. P. Garrahan, *Quantum Sci. Technol.* **4**, 02LT02 (2019).
 - [19] E. Gillman, F. Carollo, and I. Lesanovsky, *Phys. Rev. Lett.* **125**, 100403 (2020).
 - [20] E. Gillman, F. Carollo, and I. Lesanovsky, *Phys. Rev. A* **103**, L040201 (2021).
 - [21] E. Gillman, F. Carollo, and I. Lesanovsky, *Phys. Rev. Lett.* **127**, 230502 (2021).
 - [22] R. Nigmatullin, E. Wagner, and G. K. Brennen, *Phys. Rev. Res.* **3**, 043167 (2021).
 - [23] T. M. Wintermantel, Y. Wang, G. Lochead, S. Shevate, G. K. Brennen, and S. Whitlock, *Phys. Rev. Lett.* **124**, 070503 (2020).
 - [24] J. Zeiher, R. Van Bijnen, P. Schauß, S. Hild, J.-y. Choi, T. Pohl, I. Bloch, and C. Gross, *Nat. Phys.* **12**, 1095 (2016).
 - [25] H. Kim, Y. J. Park, K. Kim, H.-S. Sim, and J. Ahn, *Phys. Rev. Lett.* **120**, 180502 (2018).
 - [26] A. Browaeys and T. Lahaye, *Nat. Phys.* **16**, 132 (2020).
 - [27] S. Ebadi, T. T. Wang, H. Levine, A. Keesling, G. Semeghini, A. Omran, D. Bluvstein, R. Samajdar, H. Pichler, W. W. Ho *et al.*, *Nature (London)* **595**, 227 (2021).
 - [28] K. Beer, D. Bondarenko, T. Farrelly, T. J. Osborne, R. Salzmann, D. Scheiermann, and R. Wolf, *Nat. Commun.* **11**, 808 (2020).
 - [29] T. L. Patti, K. Najafi, X. Gao, and S. F. Yelin, *Phys. Rev. Res.* **3**, 033090 (2021).
 - [30] C. Ortiz Marrero, M. Kieferová, and N. Wiebe, *PRX Quantum* **2**, 040316 (2021).
 - [31] K. Sharma, M. Cerezo, L. Cincio, and P. J. Coles, *Phys. Rev. Lett.* **128**, 180505 (2022).
 - [32] M. Schuld and N. Killoran, *PRX Quantum* **3**, 030101 (2022).
 - [33] G. Verdon, T. McCourt, E. Luzhnica, V. Singh, S. Leichenauer, and J. Hidary, [arXiv:1909.12264](https://arxiv.org/abs/1909.12264).
 - [34] M. Broughton, G. Verdon, T. McCourt, A. J. Martinez, J. H. Yoo, S. V. Isakov, P. Massey, R. Halavati, M. Yuezhen Niu, A. Zlokapa *et al.*, [arXiv:2003.02989](https://arxiv.org/abs/2003.02989).
 - [35] J. R. McClean, S. Boixo, V. N. Smelyanskiy, R. Babbush, and H. Neven, *Nat. Commun.* **9**, 4812 (2018).
 - [36] F. Verstraete, M. M. Wolf, and J. Ignacio Cirac, *Nat. Phys.* **5**, 633 (2009).
 - [37] G. Lindblad, *Comm. Math. Phys.* **48**, 119 (1976).
 - [38] See Supplemental Material at <http://link.aps.org/supplemental/10.1103/PhysRevE.107.L022102> for details, which includes Refs. [45–48].
 - [39] K. Wiesner, Quantum cellular automata, in *Encyclopedia of Complexity and Systems Science*, edited by R. A. Meyers (Springer, New York, 2009), pp. 7154–7164.
 - [40] J. I. Cirac, D. Perez-Garcia, N. Schuch, and F. Verstraete, *J. Stat. Mech.: Theory Exp.* (2017) 083105.
 - [41] P. Arrighi, *Nat. Comput.* **18**, 885 (2019).
 - [42] T. Farrelly, *Quantum* **4**, 368 (2020).
 - [43] L. E. Hillberry, M. T. Jones, D. L. Vargas, P. Rall, N. Y. Halpern, N. Bao, S. Notarnicola, S. Montangero, and L. D. Carr, *Quantum Sci. Technol.* **6**, 045017 (2021).
 - [44] E. Chertkov, Z. Cheng, A. C. Potter, S. Gopalakrishnan, T. M. Gatterman, J. A. Gerber, K. Gilmore, D. Gresh, A. Hall, A. Hankin *et al.*, [arXiv:2209.12889](https://arxiv.org/abs/2209.12889).
 - [45] J. Eisert, *Modeling and Simulation* **3**, 520 (2013).
 - [46] S. Montangero, *Introduction to Tensor Network Methods* (Springer, Cham, 2018).
 - [47] U. Schollwöck, *Ann. Phys.* **326**, 96 (2011).
 - [48] S. Paeckel, T. Köhler, A. Swoboda, S. R. Manmana, U. Schollwöck, and C. Hubig, *Ann. Phys.* **411**, 167998 (2019).